Triplet states at an O vacancy in alpha-quartz

Lægsgaard, Jesper

Published in:
Physical Review B (Condensed Matter and Materials Physics)

Link to article, DOI:
10.1103/PhysRevB.66.024107

Publication date:
2002

Document Version
Publisher's PDF, also known as Version of record

Triplet states at an O vacancy in α-quartz

J. Lægsgaard
Research Center COM, Technical University of Denmark, Building 345v, DK-2800 Kgs. Lyngby, Denmark
(Received 5 March 2002; published 3 July 2002)

The energy landscape of an α-quartz O vacancy in the lowest triplet state is investigated. Four local minima are identified and geometries, total energies, and electron paramagnetic resonance (EPR) parameters are obtained. On the basis of calculated values for the magnetic dipole interaction between the electrons two of the structures are identified with known triplet centers detected by EPR. The effect of Ge substitution is studied, and it is concluded that Ge impurities in silica act as traps for dangling bonds with a trapping energy of ~ 1.5 eV relative to Si ions.

DOI: 10.1103/PhysRevB.66.024107 PACS number(s): 61.72.−y, 71.55.−i, 76.30.−v, 78.60.−b

I. INTRODUCTION

Refractive-index changes in silica glass induced by ultraviolet (UV) light have become an important tool in the manufacture of glass-based components for optical signal processing. Yet the origins of the effect are poorly understood and currently there is a great interest in mapping out the chemical processes occuring in undoped and doped silica under UV illumination.[1,2] A common experimental procedure has been to monitor the change in the optical and electron paramagnetic resonance (EPR) spectra as a function of UV radiation dose. One consequence of the irradiation which has been clearly established in this way is the formation of the so-called E' centers,[3] which carry both optical and EPR signatures. These centers have been well characterized, experimentally and theoretically, as arising from an unpaired spin localized in a Si dangling bond. On the basis of theoretical calculations Feigl, Fowler, and Yip[4] introduced the hypothesis that such states were created by ionization of neutral oxygen vacancies (NOV's), and this idea has been supported by several other investigations.[5,6] When an electron is removed from a NOV the Si-Si bond present is weakened, and it becomes favorable for the system to enter another state in which one of the Si atoms passes through the plane of its O neighbors and hybridizes to a fourth O atom which becomes overcoordinated. The unpaired electron will then localize in the dangling bond of the remaining threefold coordinated Si atom. Based on these results it has become a common assumption that E' center formation is related to NOV ionization, but it is often difficult to account for the fate of the expelled electrons since electronlike paramagnetic centers do not show up in the same quantity as do the E' centers.[7] In addition, recent experiments[8] indicate that E' centers may be induced through one-photon processes by UV radiation below the absorption edge, which is hard to explain if ionization of an abundant defect species is required.

An important theoretical advance was recently made by Donadio, Bernasconi, and Boero.[9] Using a combination of constrained molecular dynamics with classical forces and quantum-mechanical calculations within the framework of density functional theory (DFT) (Refs. 10,11) to model the amorphous environment in glassy SiO_2 these authors investigated the transition of a NOV geometry into a twofold coordinated Si atom in the lowest triplet state. In these studies, a competing reaction was found, in which the NOV geometry was rearranged into a structure with the two unpaired electrons residing in unhybridized dangling bonds on well-separated (4.35 Å) Si atoms. In this way, E'-like centers may be formed without ionization and a number of spectroscopic data, in particular those related to transformation of two-coordinated Si/Ge atoms, can be rationalized.

Important as these findings are, they also raise several questions. First, while the optical spectrum of a Si dangling bond would probably not be strongly perturbed by the nearby presence of another, the EPR spectrum would be characteristic of a triplet state (or, if only the singlet state is populated, would not be present at all) with strong magnetic dipole interactions which at a separation of 4–5 Å would be comparable to the hyperfine interaction with a ^{29}Si nucleus. Yet the only experimentally observed triplet state in amorphous silica was apparently related to codoping with Cl or F impurities.[12,13] One may of course speculate that the dangling bonds once separated diffuse further away from each other, but in that case how can direct experimental evidence of this reaction mechanism be obtained?

The purpose of the present work is to elucidate the possibility of E' center formation in neutral NOV's by carefully investigating the triplet energy landscape of an O vacancy in crystalline α-quartz using DFT. In α-quartz the ordered network structure greatly facilitates the comparison between theory and experiment, and several radiation-induced triplet states have been identified experimentally.[14–16] It will be shown that reactions similar to the E' generating mechanism described by Donadio *et al.* can occur in α-quartz leading to dangling-bond separations of ~ 8 Å. Through analysis of the magnetic dipole couplings between the unpaired electrons these states can be related to two of the triplet signals observed in EPR experiments. By substituting some Si atoms with Ge in the structures found it is demonstrated that Ge impurities in silica act as traps for dangling bonds with a trapping potential of ~ 1.5 eV.

II. THEORETICAL APPROACH

A. Supercell geometry

The unit cell of α-quartz is hexagonal with $a = 4.913$ Å, $c/a = 1.10$, and contains three formula units. The

crystal exist in a left-handed and a right-handed form of which I choose to model the left-handed one. The internal coordinates can be specified in terms of four parameters u,x,y,z. In Bravais vector coordinates the internal positions are

$$\mathrm{Si}_1:(u,0,0),$$

$$\mathrm{Si}_2:\left(1-u,1-u,\frac{1}{3}\right),$$

$$\mathrm{Si}_3:\left(0,u,\frac{2}{3}\right),$$

$$\mathrm{O}_1:(x,y,z),$$

$$\mathrm{O}_2:\left(1-x,y-x,\frac{1}{3}-z\right),$$

$$\mathrm{O}_3:\left(1+y-x,1-x,\frac{1}{3}+z\right),$$

$$\mathrm{O}_4:\left(y,x,\frac{2}{3}-z\right),$$

$$\mathrm{O}_5:\left(1-y,x-y,\frac{2}{3}+z\right),$$

$$\mathrm{O}_6:(1+x-y,1-y,1-z).$$

With these coordinates the c direction constitutes a left-handed threefold screw axis. The internal parameters are given by Wyckoff as $u=0.465$, $x=0.415$, $y=0.272$, $z=0.12$.[17] All calculations reported here have been performed in a supercell constructed by doubling the α-quartz unit cell in all directions, thus obtaining a cell containing 24 formula units, or 72 atoms. The internal coordinates have been allowed to relax without symmetry assumptions to minimize the DFT energy functional used, and also the lattice parameters a,c have been optimized (to $a=5.05$ Å, $c/a=1.097$). Thus, the starting point is not completely similar to the structure specified above, but it is sufficiently close that the labeling of the different atoms in the cell can still be used. I will use the notation Si_1^{ijk} to specify a Si atom equivalent to Si_1 but shifted by the vector $i\mathbf{a}_1+j\mathbf{a}_2+k\mathbf{a}_3$ where the $\mathbf{a}_i$ are the basis vectors of the Bravais lattice basis ($\mathbf{a}_3$ being the c-axis vector), and similar for the other atoms. The supercell is depicted in Fig. 1, where some important atoms have been labeled. Atoms A and B are Si_1^{000}, Si_2^{000} which are connected by O_1^{000} marked by an asterisk. This is the atom which is removed to form the O vacancy. Atom C is O_4^{010} and atom D is Si_3^{010}. The importance of these latter atoms will become apparent in Sec. III A.

B. Computational methods

The electronic structure of the system is described by means of DFT using the generalized gradient approximation (GGA) to the exchange-correlation energy.[18] The resulting Kohn-Sham equations are solved by means of a plane-wave expansion using Vanderbilt's ultrasoft pseudopotential (US-PP) approach.[19,20] In all calculations, the plane-wave expansion is cut off at a kinetic energy of 25 Ryd, and the Brillouin zone integrations are approximated by sampling the Γ-point only.

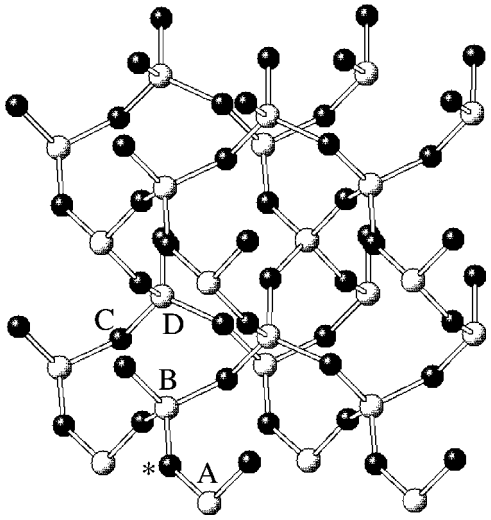

FIG. 1. The 72-atom α-quartz supercell used in the present work. White atoms are Si while black atoms are O. In the calculations, the atom marked with an asterisk is removed to form an O vacancy. Atoms A,B,C,D correspond to Si_1^{000}, Si_2^{000}, O_4^{010}, Si_3^{010}, respectively.

The calculation of hyperfine parameters requires knowledge of the wavefunction close to, or even right at, the nucleus, which appears to present a problem, since the pseudopotentials do not describe the wave function correctly in this region of space. To overcome this problem, I reconstruct the true wavefunction in the core region by augmenting the pseudo wave function along the lines described in Ref. 21. Using this procedure, one obtains a wavefunction very similar to that of the projector augmented wave scheme introduced by Blöchl,[22,23] which has been shown to give rather accurate results for the properties of interest here.[24–26] For the isotropic part of the hyperfine tensor, core polarization effects are approximately taken into account by recalculating the core states while keeping the spin-polarized valence electron density fixed. This is not an exact approach, as it ignores the back reaction of the core spin polarization on the valence electron density, but it serves to give an idea of the magnitude of the core polarization effect. In the present case, core polarization was found to affect the isotropic hyperfine parameters by about 1–2 % in the case of ^{29}Si, ^{73}Ge whereas in the case of ^{17}O the correction in some cases amount to about 20%.

A significant contribution to the EPR spectra of triplet states comes from the magnetic dipole interaction between the two electrons. This interaction may formally be written as

$$\hat{H}_d=\hat{\mathbf{S}}_1\cdot\mathbf{D}\cdot\hat{\mathbf{S}}_2, \tag{1}$$

where $\hat{\mathbf{S}}_1, \hat{\mathbf{S}}_2$ are the vector spin operators for electrons 1 and 2 and **D** is a tensor defined by

$$D_{\mu\nu} = \frac{1}{2} g^2 \beta^2 \left\langle \hat{S}_{1\mu} \hat{S}_{2\nu} \frac{3 r_\mu r_\nu - \delta_{\mu\nu} r^2}{r^5} \right\rangle. \tag{2}$$

Here the greek indices label cartesian directions, $\mathbf{r} = \mathbf{r}_1 - \mathbf{r}_2$ and $r = |\mathbf{r}|$ is the distance between electrons 1 and 2. g is the electron g factor (≈ 2.0023 for a free electron) while β is the electron magnetic moment. The brackets denote an expectation value over the many-electron wave function. If the unpaired spins reside at spatially well separated defect sites only the mean-field term survives

$$D_{\mu\nu} \approx \frac{1}{2} g^2 \beta^2 \int d\mathbf{r}_1 d\mathbf{r}_2 \frac{n_1(\mathbf{r}_1) n_2(\mathbf{r}_2)(3 r_\mu r_\nu - \delta_{\mu\nu} r^2)}{r^5}. \tag{3}$$

In this formula, n_1, n_2 are the spin densities at defects 1 and 2. The spin density in the lowest triplet state is given correctly by an exact density functional theory, whereas this is not the case for the off-diagonal parts of the density matrix which would be needed to evaluate the short-range exchange corrections. In the present work the dipole interaction tensor will be approximated by Eq. (3). If the defects are far from each other their spin densities may be approximated by point dipoles and the **D** tensor will be proportional to r^{-3}. However, at intermediate distances, the finite spatial extent of the spin densities can give substantial corrections to this picture, and must be taken into account. The evaluation of the integral in Eq. (3) directly from the supercell spin densities is subject to errors arising from the finite supercell size and the resulting presence of repeated-image spin densities. A similar problem is encountered when describing charged states in a supercell approach, although in the magnetic case the leading error term decays with the cube of the lattice constant. For isolated molecules a method for eliminating interactions with repeated images has been devised by Blöchl,[27] but this is not straightforwardly extended to solids. To work around this problem, for each defect site a small cluster model including only a few atoms is set up based on the coordinates obtained in the supercell calculations. The resulting spin densities are then immersed in a supercell eight times larger than the one used for the DFT calculations and the integral in Eq. (3) is evaluated in reciprocal space. Errors arising from the dipole moments of repeated images in the enlarged cell can now be eliminated by Blöchl's procedure since the spin densities are well localized within the supercell. By further enlarging the cell it was found that the errors arising from higher-order moments of the image spin distributions were minute. Although the approach described implies some inaccuracies it still constitutes a considerable improvement over the point dipole approximation.

III. NUMERICAL RESULTS

A. Total energies and geometric structures

Without spin polarization, the removal of O_1^{000} leads to the formation of a covalent bond between Si_1^{000} and Si_2^{000}. In the present calculation the equilibrium bond length comes out as 2.50 Å, which is in good agreement with results from other similar studies.[6,26,9] Going into the triplet state in this equilibrium structure implies the population of one bonding and one antibonding Si-Si state, i.e., a breaking of the covalent Si-Si bond. The penalty for this is calculated to be 5.6 eV. Since DFT in principle gives the true ground-state energy for every value of the total spin, this number constitutes a physical prediction of the GGA approximation. Experimentally, the lowest singlet-triplet transition is not observable, however, some elaborate theoretical studies have been performed by configuration-interaction (CI) calculations on small cluster models. Such calculations have predicted the lowest singlet-singlet transition in the system (which is observed experimentally) with good accuracy.[28] Predictions for the singlet-triplet excitation have varied between 6.2 and 6.9 eV depending on the computational details.[28,29] This suggests that the GGA result underestimates the singlet-triplet transition energy by 10–20 %.

In the triplet state, the system initially relaxes to a new equilibrium configuration in which the Si-Si distance expands to 3.56 Å. The geometry, hereafter denoted T_I, is shown in Fig. 2(a). The Si-Si distance is considerably larger than that found by Busso *et al.*[30] who concluded that the Si-Si distance was close to the value for the unrelaxed α-quartz structure (~ 3.1 Å). On the other hand, the present result is close to the 3.69 Å found from Hartree-Fock calculations on a small cluster model by Pacchioni and Basile.[29] These authors reported a triplet-singlet decay energy of 0.57 eV when doing CI calculations in the Hartree-Fock equilibrium geometry, indicating that this decay cannot be responsible for the 2.7 eV luminescence observed to follow from NOV excitation.[31] In the present calculations, the triplet-singlet decay energy is ~ 1.5 eV, but this is likely to be an artifact of the GGA approximation: When the Si-Si bond is stretched the system starts to resemble a Hubbard model with a small hopping parameter. In such a problem hybridization is suppressed by the onsite electron-electron repulsion but this correlation effect is hard to capture with simple DFT energy functionals. Therefore, it must be expected that the singlet state energy is underestimated in DFT, yielding a too large value for the decay energy. The important result of the DFT calculation is the Si-Si distance in the triplet equilibrium geometry, since structural relaxations are better described in the supercell than in the small cluster model. Therefore, the present results support the conclusion of Pacchioni and Basile regarding the assignment of the 2.7 eV luminescence.

The existence of a second energy minimum in the triplet state was recently reported by Busso *et al.*[30] These authors used a perturbed cluster (PC) approach which embeds a central cluster of atoms surrounding the defect in an unperturbed crystal medium employing a Hartree-Fock energy functional with *a posteori* DFT-like correlation corrections. Only the positions of the first and second nearest neighbor shells to the O vacancy were relaxed. With this scheme, a minimum was found in which the Si_2^{000} atom has passed through the plane defined by its three O neighbors into a ''puckered'' configuration. A similar minimum is found in the present

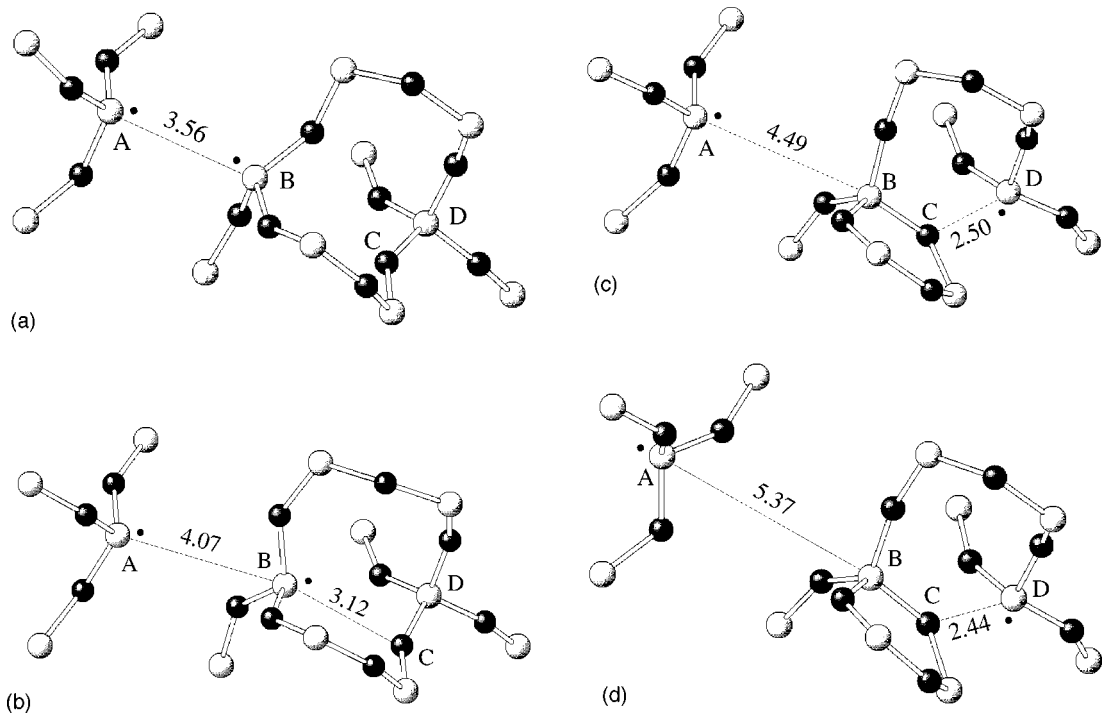

FIG. 2. The stable triplet geometries identified in the present work. (a)–(d) show structures T_{I}–T_{IV}. Some distances are given in Å, and the labeling from Fig. 1 has been used so that A, B, C, D corresponds to Si_1^{000}, Si_2^{000}, O_4^{010}, Si_3^{010}, respectively. The small black circles indicate the locations of the unpaired spins.

work, as shown in Fig. 2(b). This geometry will be referred to as T_{II}. The total energy of T_{II} is 0.25 eV lower than that of T_{I}, in very good agreement with the 0.3 eV found by Busso *et al.* The distance between Si_1^{000} and Si_2^{000} is now 4.07 Å and the Si_2^{000} atom has moved within a distance of 3.12 Å of O_4^{010} (labeled C in the figures). The Si-Si distance is in good accordance with the results of Busso *et al.*, whereas the distance from Si_2^{000} to O_4^{010} is somewhat larger here, presumably due to the higher degree of relaxational freedom.

The T_{II} structure also constitutes a local minimum in the singlet state, with localized antiparallel spins at the Si_1^{000} and Si_2^{000} atoms. The singlet-triplet energy difference is only $\sim$0.05 eV (in favor of the singlet state). It is not clear how reliable the GGA approximation is in predicting such singlet-triplet energy differences, but the result does indicate that very little interaction between the Si dangling bonds remains.

Using the geometry of a positively charged E' center as a starting point for relaxations in the neutral triplet state another pair of local minima were identified. These are depicted in Figs. 2(c), 2(d) and will be denoted T_{III} and T_{IV}, respectively. The bond between O_4^{010} and Si_2^{000} present in the charged E' center geometry has remained, whereas the bond between O_4^{010} and Si_3^{010} is broken. As a result, comparing T_{II} to T_{III}, T_{IV} the dangling bond has been transferred from Si_2^{000} to Si_3^{010} and at the same time a three-membered ring structure has been formed. T_{III} and T_{IV} are distinguished by the position of Si_1^{000} which is shifted through the plane of its nearest O neighbors when going from T_{III} to T_{IV}. The total energies of T_{III}, T_{IV} are, respectively, 0.8 and 1.0 eV higher than that of T_{II} which constitutes the energy minimum for the equilibrium geometries found. While it is not unreasonable that increased lattice strain, in particular the formation of a three-membered ring structure, will disfavor the T_{III} and T_{IV} geometries it is important to bear in mind the limitations of the supercell approach. Quite generally, the use of a finite supercell leads to overestimation of defect formation energies due to the limited number of relaxational degrees of freedom. When the energies of different defect structures in the same supercell are compared these errors will cancel to some extent, but since complex reconstructions are likely to require more relaxation of the surrounding network such states will be disfavoured by the supercell approach in comparison with simpler geometries. T_{III} and, in particular, T_{IV} are on the limit of what can be reliably modeled in a 72-atom α-quartz cell. The distance from Si_1^{000} to Si_3^{010} in the T_{III} (T_{IV}) geometry is $\sim$7.7(8.5) Å, whereas the distance from Si_3^{010} to the nearest repeated image of Si_1^{000} is only $\sim$5.8(5.5) Å. There is no appreciable electronic interaction with the repeated images since the dangling bonds do not point towards each other. This is evidenced by the small energy differences between singlet and triplet states in these geometries (0.04 eV for T_{III} and 0.007 eV for T_{IV}). However, the elastic interactions with the image may lead to errors in the relative energies of the defect structures of a considerable fraction of an eV, and therefore the energy difference between T_{II} and T_{III}, T_{IV} may be somewhat overestimated here.

It is interesting to notice that the total-energy results of Donadio *et al.* are quite different from those obtained here in that these authors found the state with separated dangling

bonds (i.e., the equivalent of $T_{\mathrm{III}}, T_{\mathrm{IV}}$) to be *favored* over the ordinary NOV structure (relaxed in the triplet state) by as much as 1.6 eV.[9] Such a large difference is unlikely to be caused solely by the limited relaxational freedom, in particular since Donadio and co-workers also utilized a supercell approach (albeit with a slightly larger cell). This shows that the local environment around the NOV plays a decisive role in determining the relative energies of the various geometries, so a careful investigation of amorphous environments will be needed to elucidate the importance of similar states in silica glass.

B. EPR parameters

The most important parameters for identification of the triplet states with spectroscopic signals are the magnetic dipole-dipole couplings between the unpaired electrons since these depend strongly on the distance and relative orientation of the two unpaired spins whereas the hyperfine couplings are more indicative of the shape of each spin distribution close to the magnetic nucleus. As explained in Sec. II B the dipole-dipole coupling parameters are evaluated from the spin distributions of small cluster models set up by cutting out each of the three-coordinated Si atoms and its nearest O neighbors from the relaxed supercell geometries. The next-nearest (Si) neighbors are replaced by H atoms and are drawn towards the O atoms to a distance of 0.98 Å keeping the bond directions fixed. The cluster models for Si_1^{000} and Si_3^{010} in the T_{IV} geometry are shown in Fig. 3. For the Si_2^{000} atom in T_{II} and the Si_3^{010} atom in T_{III}, T_{IV} the O_4^{010} atom has been included in the cluster model as shown in Fig. 3(b). The hyperfine parameters obtained for the Si nuclei are within $\sim$20% of the supercell results showing that the wave function shapes are reasonably well reproduced. The principal values and directions for the dipole-dipole tensors found are given in Table I. The principal values have been converted to units of Gauss (G) by dividing by $g\beta$.

The effect of the dipole-dipole interaction at zero magnetic field is to split the otherwise degenerate triplet levels, and at finite field to shift the Zeeman levels so that the two $\Delta m = 1$ transitions do not have exactly the same energy. In EPR experiments, Zeeman transitions are usually induced by microwave photons of a fixed frequency while the uniform magnetic field is scanned over a range of values in search of microwave absorption peaks. If the dipole-dipole coupling is weak compared to the Zeeman splitting, as is usually the case, a triplet state will appear as a pair of nearby resonance lines. The distance between the lines depends on the orientation of the uniform magnetic field relative to the principal directions of the **D** tensor. For an axially symmetric tensor it can be shown that the maximum observable splitting is three times the principal value along the symmetry axis.

Experimentally, several triplet centers in irradiated α-quartz samples have been identified over the years.[32,15,16] The nature of the centers seems to depend on the nature of the radiation. In light of the results for T_{III} and T_{IV} reported in Table I the centers found by Bossoli, Jani, and Halliburton[15] in electron-irradiated α-quartz seem particularly interesting. Working with a microwave frequency of 9.3165 GHz and a magnetic field oriented along the c axis these authors identified three triplet centers with line separations of 5, 11, and 18 G, respectively. These centers are commonly labeled E_1'', E_2'', E_3''. Rotating the magnetic field in the plane perpendicular to the crystallographic $\mathbf{a}_1$ axis the centers showed maximum peak separations of 192 G for E_1'',

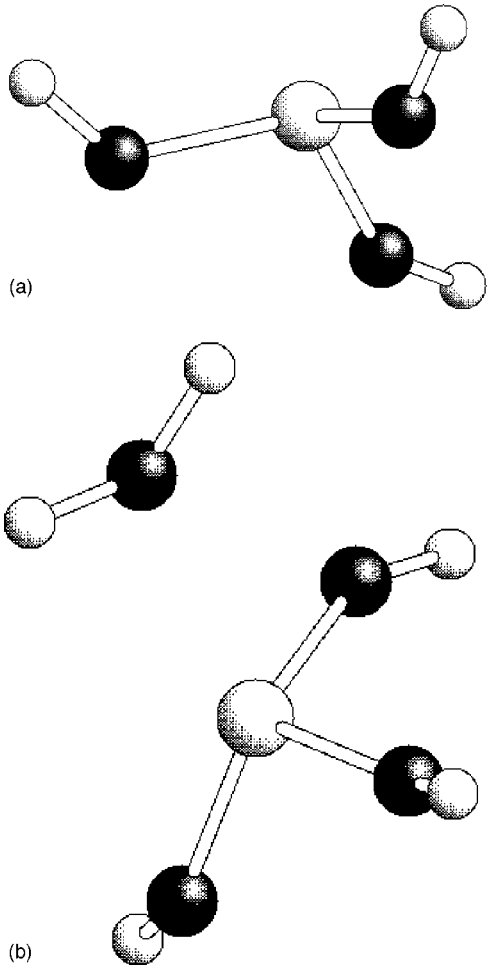

FIG. 3. Cluster models used for calculating the electron magnetic-dipole interactions in T_{IV}. In (a) the model for Si_1^{000} is shown, while the model for Si_2^{000} (note the inclusion of O_4^{010}) is depicted in (b). The small white spheres represent the saturating H atoms.

TABLE I. Principal values (in gauss) and directions for the dipole-dipole tensor in the T_{II}, T_{III}, and T_{IV} geometries. The principal directions are given by their polar angles around the c axis.

State	Princ. values			Princ. directions		
	P_1	P_2	P_3	θ_1, ϕ_1	θ_2, ϕ_2	θ_3, ϕ_3
T_{II}	-218	99	119	$\theta = 124°$	$\theta = 48°$	$\theta = 61°$
				$\phi = 283°$	$\phi = 336°$	$\phi = 216°$
T_{III}	-54	26	28	$\theta = 127°$	$\theta = 136°$	$\theta = 70°$
				$\phi = 259°$	$\phi = 63°$	$\phi = 355°$
T_{IV}	-25	11	13	$\theta = 51°$	$\theta = 55°$	$\theta = 58°$
				$\phi = 111°$	$\phi = 235°$	$\phi = 351°$

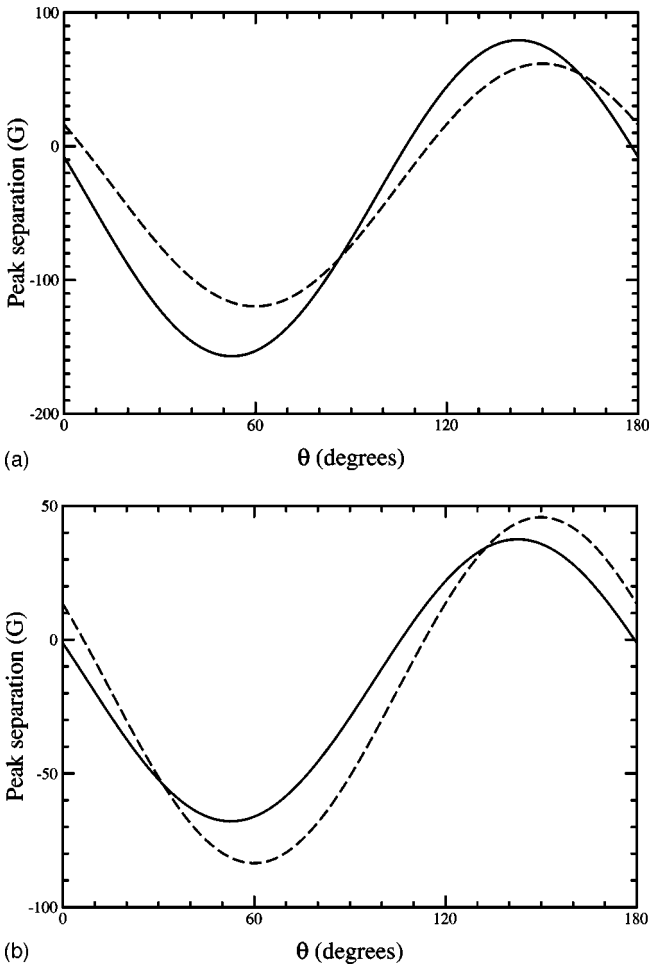

FIG. 4. Calculated triplet peak separations under rotation of the magnetic field in the plane perpendicular to $\mathbf{a}_1$. Solid lines give the results obtained from the parameters in Table I, while the dashed lines give the results of the point dipole approximation. The angle is measured relative to the *c* axis.

64 G for E_2'', and 51 G for E_3''. Comparing these results with the principal values in Table I, T_{III} and T_{IV} appear to be candidates for E_1'' and E_2'', respectively. In order to investigate this hypothesis further, a simulation of the EPR experiment was performed using the calculated parameters for the magnetic-dipole coupling. To account for the threefold screw symmetry along the *c*-axis rotation of the magnetic field in the plane perpendicular to $\mathbf{a}_1$ as well as in planes rotated 120° clockwise and counterclockwise around the *c* axis was considered. The largest peak separations were in both cases found in the plane perpendicular to $\mathbf{a}_1$. In Fig. 4 the resulting peak separation is shown as a function of the magnetic field orientation relative to the *c* axis. The sign of the separation is an arbitrary choice which has no bearing on the experimental signal. For T_{III}, the peak separation with the field parallel to the *c* axis is found to be 8 G and the maximum peak separation is 157 G. For T_{IV}, the values are 1.3 and 68 G. Thus the maximum peak separations are in reasonably good agreement with the experimental values and also the comparatively small peak separation with a *c*-parallel magnetic field is qualitatively reproduced here. For T_{IV}, the quantitative agreement between theory and the experimental signal is less satisfactory at this field orientation, but as can be seen from Fig. 4, the variation of the peak separation with field angle is steep here and small errors in the relative orientation of the spin densities can significantly affect the results. I will therefore tentatively assign the signals E_1'' and E_2'' to the triplet geometries T_{III} and T_{IV} on the basis of the above results.

TABLE II. Hyperfine parameters (in Gauss) for some ^{29}Si and ^{17}O centers in the T_{II}, T_{III}, and T_{IV} geometries. Only the isotropic coupling, A_{iso} and the largest component of the anisotropic matrix $A_{||}$ are given.

Atom	A_{iso}			$A_{||}$		
	T_{II}	T_{III}	T_{IV}	T_{II}	T_{III}	T_{IV}
Si_1^{000}	−488	−477	−405	−51	−50	−51
Si_2^{000}	−434	−8	−12	−50	−1	−1
Si_3^{010}	0	−555	−545	0	−48	−47
O_4^{010}	−14	−67	−70	−6	−12	−12

Also shown in Fig. 4 are the predictions of the point dipole approximation, assuming the spin density distributions of the unpaired electrons to be delta functions at the positions of Si_1^{000} and Si_3^{010}. It is evident that the finite extent of the spin densities has a significant influence on the results. Note in particular that the difference in magnitude of the dipole couplings between T_{III} and T_{IV} is much smaller in the point dipole approximation. This is due to the fact that the change in position of Si_1^{000} between the two states also affects a flipping of the direction of the orbital in which the unpaired spin resides. Thus, when going from T_{III} to T_{IV} the electronic spin densities are moved further apart from each other than the atomic coordinates reveal. The identification of T_{III}, T_{IV} with the E_1'' and E_2'' centers would appear much more dubious from the point dipole results alone. This clearly demonstrates the importance of accounting for the spin density shape at intermediate distances between defects. Note also the relatively large discrepancy between the two approximations at $\theta = 0$.

Hyperfine parameters calculated for ^{29}Si nuclei at the Si_1^{000}, Si_2^{000}, and Si_3^{010} positions, as well as ^{17}O at the position of O_4^{010} are given in Table II in units of Gauss. The anisotropic tensors have approximately axial symmetry and therefore only the component of largest magnitude ($A_{||}$) has been given. The isotropic coupling is determined by the *s* component of the wave function right at the nucleus, while the magnitude of the anisotropic tensor roughly follows the occupation of the *p* states. Therefore, contrary to what one might naively expect, the anisotropic tensor constitutes the better measure of spin occupancy at a particular atom, whereas the isotropic coupling is more indicative of wave function shape (*s*-*p* hybridization). The hyperfine parameters have been calculated for the T_{II}, T_{III}, and T_{IV} geometries since these can be expected to be stable enough to be observable, at least at low temperatures. The lifetime of the T_{I} state will be on the order of miliseconds since the bond between Si_1^{000} and Si_2^{000} will immediately reform when the system reverts back into the singlet state. The hyperfine parameters

in Table II clearly show that one of the unpaired spins is transferred from Si_2^{000} to Si_3^{010} when going from T_{II} to T_{III}. In the former geometry, the spin density at Si_3^{010} is vanishingly small, whereas the hyperfine parameters of Si_2^{000} are comparable to those of the α-quartz E' center. For T_{III}, the situation is reversed. In both structures an unpaired electron is present at Si_1^{000} whose hyperfine interactions are virtually unaffected by the transition between T_{II} and T_{III}. Going from T_{III} to T_{IV}, on the other hand, affects a significant reduction of the isotropic part of the Si_1^{000} hyperfine matrix while the Si_3^{010} parameters are similar in the two structures.

When looking at Fig. 2(c) it is at once evident that the Si nuclei at which the two spins are centered (atoms A and D in the figure) are not completely equivalent: Atom D (Si_3^{010}) is electrostatically attracted towards atom C (O_4^{010}) and the separation of these ions in the equilibrium geometry is only 2.44 Å. This difference is also reflected in the values of the hyperfine parameters. The magnitude of the anisotropic tensor is reduced at Si_3^{010} compared with Si_1^{000}, Si_2^{000} suggesting that some spin weight is transferred to O_4^{010}. It can be seen from the O_4^{010} hyperfine parameters that the spin density at this nucleus grows when the dangling bond is transferred from Si_2^{000} to Si_3^{010}. The isotropic hyperfine parameter of Si_3^{010} is significantly larger than those of Si_1^{000} and Si_2^{000}, indicating greater *s*-*p* hybridization in this case.

The presence of a hyperfine nucleus at a triplet center leads to a splitting of the signal into two doublets whose separation reflects the magnitude of the hyperfine couplings. Since the ^{29}Si nucleus is only 5% abundant the dominant hyperfine signal comes from states in which only one magnetically active nucleus is present at a triplet center. In the T_{III} state the hyperfine parameters found here predict a splitting between doublets of 230 G if the magnetic nucleus is at the position of Si_1^{000} and 287 G if it is at the Si_3^{010} position. Experimentally, Bossoli *et al.* found splittings of 195 and 203 G for the E_1'' center. For E_2'' the reported splittings were 170–185 and 209 G whereas the present calculations predict 197 and 275 G, respectively. Although the magnitude of the hyperfine couplings are somewhat overestimated by the theory, the reduction of the Si_1^{000} value for A_{iso} when going from T_{III} to T_{IV} is clearly reflected in the experimental results.

The experimental value of A_{iso} for an ordinary E' center is 412 G,[33] but theoretical studies using a pseudopotential method similar to the one employed here predicted a value of 468 G,[6] close to the results found in the present work for Si_1^{000} in the T_{II} and T_{III} states. Therefore it seems likely that the Si_1^{000} A_{iso} parameter is similar to the ordinary E' center value in states T_{II}, T_{III} but has a smaller value in the T_{IV} structure. In crystalline quartz the doublet spectrum of the E' state can be clearly distinguished from the spectra of the triplet states discussed here, so the present results are of no consequence for the interpretation of the ordinary E' signal. In amorphous silica the interpretation of experimental data is less straightforward, and one can speculate that the observed E' spectra may have contributions from states similar to T_{II}-T_{IV} or the geometry described by Donadio *et al.*[9] Such a signal would be broadened by the dipole-dipole interactions due to the random orientation of the dipole-dipole coupling tensor, so a state with a spin separation of 4-5 Å would be practically invisible in EPR (but not in optical) spectroscopy. States with intermediate separation, such as T_{III} and T_{IV}, would lead to a somewhat larger signal broadening than observed experimentally,[34] meaning that such states cannot contribute strongly to the spectra. However, at separations beyond 15–20 Å the dipole-dipole broadening would be hard to distinguish, so further diffusion of dangling bonds in the amorphous network is a possibility that cannot immediately be ruled out. The broadening of the hyperfine doublet of $\sim$50 G observed in amorphous silica[34] is reasonably consistent with the spread in the hyperfine parameters calculated here, but of course this does not prove the diffusion hypothesis as it could also be caused by the structural disorder in other ways.

C. Effect of Ge substitution

Since the refractive-index changes attainable by UV irradiation of silica glass are greatly increased by Ge doping it is important to understand how E' center formation is influenced by Ge impurities. It is usually assumed that Ge doping stabilizes the formation of O vacancies since the *sp* levels of Ge are slightly lower in energy than those of Si, and also that Ge impurities and O vacancies/dangling bonds are attracted to each other. In order to estimate the attraction strength between dangling bonds and Ge impurities and compare Ge hyperfine parameters for the two E' center variants discussed in the previous section, the T_I, T_{II}, and T_{IV} geometries were reoptimized after substituting Si_1^{000} and Si_3^{010} by Ge. In all cases local minima corresponding to those in pure α-quartz were found also in the Ge-doped case. In analogy with the above, I will denote these geometries T_I^{Ge}, T_{II}^{Ge}, and T_{IV}^{Ge}, and the substituting Ge ions Ge_1^{000}, Ge_3^{010}. The T_{II}^{Ge} configuration is 0.07 eV lower in energy than T_I^{Ge}, showing that the Ge substitution does not greatly affect the energy difference between these two states. It is, however, interesting to note that Busso *et al.* found the opposite trend, i.e., stabilization of the T_{II} state upon Ge substitution of Si_1^{000} only. Whether this is due to the technical differences between the two calculations or the influence of Ge_3^{010} in the present calculation is not clear. The main effect of Ge_3^{010}, however, is to stabilize the T_{IV}^{Ge} state, compared to T_I^{Ge}, T_{II}^{Ge}. The energy of T_{IV}^{Ge} is found to be 0.61 eV lower than that of T_{II}^{Ge}. Comparing to the pure Si case in which T_{IV} was disfavored by 0.75 eV compared to T_I and 1.0 eV compared to T_{II} this shows that the transfer of a dangling bond from Si to Ge gains about 1.5 eV all other things being equal.

The hyperfine parameters calculated for the Ge impurities are given in Table III. The trends observed for the Ge impurities are similar to the pure SiO_2 case. However, the perturbation of the Ge signals by the proximity to O_4^{010} in T_{IV} is considerably larger than in the Si case. This is presumably due to the larger radius of the Ge wave functions. This is also reflected in a considerably larger spin density at the O_4^{010} nucleus, as seen from the increased magnitude of the aniso-

TABLE III. Hyperfine parameters (in Gauss) for some ^{29}Si, ^{73}Ge , and ^{17}O centers in the $T_{\mathrm{II}}^{\mathrm{Ge}}$ and $T_{\mathrm{IV}}^{\mathrm{Ge}}$ geometries. Only the isotropic coupling, A_{iso} and the largest component of the anisotropic matrix $A_{||}$ are given.

Atom	A_{iso}		$A_{\|\|}$	
	$T_{\mathrm{II}}^{\mathrm{Ge}}$	$T_{\mathrm{IV}}^{\mathrm{Ge}}$	$T_{\mathrm{II}}^{\mathrm{Ge}}$	$T_{\mathrm{IV}}^{\mathrm{Ge}}$
Ge_1^{000}	−313	−259	−19	−19
Si_2^{000}	−443	−4	−49	−1
Ge_3^{010}	−2	−407	0	−15
O_4^{010}	−31	−63	−9	−16

tropic hyperfine tensor. Experimentally, no Ge signals from E''-like states have been reported, and in general Ge hyperfine splittings are rarely resolved due to the high ($I=\frac{9}{2}$) value of the ^{73}Ge nuclear spin. Feigl and Anderson reported two signals appearing to be variants of a Ge-related E' center in Ge-doped α-quartz . The isotropic hyperfine parameters were 234 and 268 G (218 and 250×10^{-4} cm^{-1}).[35] Watanabe *et al*. reported a value of 251 G for a silica fiber.[36] Again it must be stressed that the geometries investigated in the present work do not constitute proper models of a doublet E' center. Nevertheless it is interesting to notice that these experimental values correspond reasonably well with the theoretical results for Ge_1^{000} in the $T_{\mathrm{II}}^{\mathrm{Ge}}$ and $T_{\mathrm{IV}}^{\mathrm{Ge}}$ geometries, especially when considering that the present approach tended to overestimate the ^{29}Si isotropic couplings somewhat. Thus it is possible that the two E' center variants observed transform into each other by passing the threefold coordinated Ge atom through the plane of its nearest neighbors. There are, however, other possible interpretations (such as the substitutional Ge being present at either the long- or short-bonded side of the O vacancy) and direct modeling of the doublet-state geometry will be needed to resolve the issue. In addition, it should be noted that there are some technical issues to be sorted out in connection with the calculation of ^{73}Ge hyperfine parameters: Pacchioni and Mazzeo[37] have recently reported that cluster model calculations using a Gaussian basis set and Hartree-Fock or combined Hartree-Fock-DFT energy functionals predicted isotropic hyperfine parameters of 164–192 G, thus underestimating the experimental values considerably in contrast to the overestimation found in the present work.

IV. CONCLUSIONS

The triplet-state energy landscape of a neutral oxygen vacancy in α-quartz has been investigated and four different local minima have been identified. Dipole-dipole couplings between the unpaired electrons and hyperfine interactions with ^{29}Si and ^{17}O nuclei have been calculated and related to EPR experiments. Two triplet signals observed experimentally are in this way assigned to two of the metastable geometries found in the theoretical calculations. This provides experimental support for the idea that the Si dangling bonds around an O vacancy can be widely separated from each other through structural reconstructions. By substituting Ge atoms into some of the structures it is demonstrated that substitutional Ge impurities act as traps for dangling bonds in a silica network with a trapping potential of about 1.5 eV.

ACKNOWLEDGMENTS

The author wishes to acknowledge Professor Martin Kristensen for valuable discussions and a critical reading of the manuscript. The use of Danish national computer resources was supported by the Danish Research Council.

[1] R. Kashyap, *Fiber Bragg Gratings* (Academic Press, San Diego, 1999).
[2] M. Kristensen, Phys. Rev. B **64**, 144201 (2001).
[3] R.A. Weeks, J. Non-Cryst. Solids **179**, 1 (1994).
[4] F.J. Feigl, W.B. Fowler, and K.L. Yip, Solid State Commun. **14**, 225 (1974).
[5] J.K. Rudra and W.B. Fowler, Phys. Rev. B **35**, 8223 (1987).
[6] M. Boero, A. Pasquarello, J. Sarnthein, and R. Car, Phys. Rev. Lett. **78**, 887 (1997).
[7] M. Fujimaki, T. Katoh, T. Kasahara, N. Miyazaki, and Y. Ohki, J. Phys.: Condens. Matter **11**, 2589 (1999).
[8] Y. Ikuta, S. Kikugawa, M. Hirano, and H. Hosono, J. Vac. Sci. Technol. B **18**, 2891 (2000).
[9] D. Donadio, M. Bernasconi, and M. Boero, Phys. Rev. Lett. **87**, 195504 (2001).
[10] P. Hohenberg and W. Kohn, Phys. Rev. **136**, B864 (1964).
[11] W. Kohn and L. Sham, Phys. Rev. **140**, A1133 (1965).
[12] D.L. Griscom and E.J. Friebele, Phys. Rev. B **34**, 7524 (1986).
[13] R. Tohmon, Y. Shimogaichi, Y. Tsuta, S. Munekuni, Y. Ohki, Y. Hama, and K. Nagasawa, Phys. Rev. B **41**, 7258 (1990).
[14] R.A. Weeks and M. Abraham, J. Appl. Phys. **56**, 942 (1984).
[15] R.B. Bossoli, M.G. Jani, and L.E. Halliburton, Solid State Commun. **44**, 213 (1982).
[16] M.G. Jani and L.E. Halliburton, J. Appl. Phys. **56**, 942 (1984).
[17] R.W.G. Wyckoff, *Crystal Structures* (Interscience, New York, 1965).
[18] D.C. Langreth and M.J. Mehl, Phys. Rev. B **28**, 1809 (1983); J.P. Perdew and Y. Wang, *ibid.* **33**, 8800 (1986); J.P. Perdew, *ibid.* **33**, 8822 (1986).
[19] D. Vanderbilt, Phys. Rev. B **41**, 7892 (1990).
[20] K. Laasonen, A. Pasquarello, R. Car, C. Lee, and D. Vanderbilt, Phys. Rev. B **47**, 10 142 (1993).
[21] J. Lægsgaard and K. Stokbro, Phys. Rev. B **63**, 075108 (2001).
[22] P.E. Blöchl, Phys. Rev. B **50**, 17 953 (1994).
[23] G. Kresse and D. Joubert, Phys. Rev. B **59**, 1758 (1999).
[24] C.G. VandeWalle and P.E. Blöchl, Phys. Rev. B **47**, 4244 (1993).
[25] H.M. Petrilli, P.E. Blöchl, P. Blaha, and K. Schwarz, Phys. Rev. B **57**, 14 690 (1998).
[26] P.E. Blöchl, Phys. Rev. B **62**, 6158 (2000).
[27] P. Blöchl, J. Chem. Phys. **103**, 7422 (1995).
[28] G. Pacchioni and G. Ieranò, Phys. Rev. Lett. **79**, 753 (1997).
[29] G. Pacchioni and A. Basile, J. Non-Cryst. Solids **254**, 17 (1999).

[30] M. Busso, S. Casassa, C. Pisani, and V.B. Sulimov, Modell. Simul. Mater. Sci. Eng. **10**, 21 (2002).
[31] L. Skuja, J. Non-Cryst. Solids **149**, 77 (1992).
[32] R.A. Weeks and M. Abraham, Bull. Am. Phys. Soc. **10**, 374 (1965).
[33] M.G. Jani, R.B. Bossoli, and L.E. Halliburton, Phys. Rev. B **27**, 2285 (1983).
[34] D.L. Griscom, E.J. Friebele, and G.H. S., Jr., Solid State Commun. **15**, 479 (1974).
[35] F.J. Feigl and J.H. Anderson, J. Phys. Chem. Solids **31**, 575 (1970).
[36] Y. Watanabe, H. Kawazoe, K. Shibuya, and K. Muta, Jpn. J. Appl. Phys., Part 1 **25**, 425 (1986).
[37] G. Pacchioni and C. Mazzeo, Phys. Rev. B **62**, 5452 (2000).